ELSEVIER

Surface Science 410 (1998) 151–157

surface science

The reconstruction of Rh(001) upon oxygen adsorption

D. Alfè [a,*1], S. de Gironcoli [a], S. Baroni [a,b]

[a] *INFM – Istituto Nazionale di Fisica della Materia and SISSA – Scuola Internazionale di Studi Superiori ed Avanzati, via Beirut 2–4, I-34014 Trieste, Italy*

[b] *CECAM, ENSL, Aile LR5, 46 Allée d'Italie, F-69364 Lyon, Cedex 07, France*

Received 24 October 1997; accepted for publication 19 January 1998

Abstract

We report on a first-principles study of the structure of O/Rh(001) at half a monolayer of oxygen coverage, performed using density functional theory. We find that oxygen atoms sit at the center of the black squares in a chess-board $c(2\times2)$ pattern. This structure is unstable against a rhomboid distortion of the black squares, which shortens the distance between an O atom and two of the four neighboring Rh atoms, while lengthening the distance with respect to the other two. We actually find that the surface energy is further lowered by allowing the O atom to get off the short diagonal of the rhombus thus formed. We predict that the latter distortion is associated with an order–disorder transition, occurring below room temperature. The above rhomboid distortion of the square lattice may be seen as a rotation of the empty white squares. Our findings are at variance with recent claims based on STM images, according to which it is instead the black squares which would rotate. We argue that these images are indeed compatible with our predicted reconstruction pattern.

Keywords: Chemisorption; Density functional calculations; Oxygen; Rhodium

1. Introduction

The study of the physical and chemical properties of the (001) surface of rhodium is an important step towards the ambitious goal of understanding the catalytic properties of transition metals. Recently, the clean Rh(001) surface has attracted experimental [1–3] and theoretical [4–9] interest because of the anomalously small interlayer relaxation at the surface, an unexpected result which is in contrast with the general behavior of transition-metal surfaces. One more reason of interest is due to the behavior of the surface upon oxygen adsorption. Oxygen adsorption on Rh(001) is known to be dissociative and to saturate at half a monolayer, independently of the adsorption temperature. At this coverage, a (2×2) reconstruction has been observed by SPA-LEED and confirmed by STM [10]. The oxygen atoms sit in the troughs formed by four first-layer rhodium atoms and fill these sites in a $c(2\times2)$ geometry. This geometry may be considered as a chess-board whose black squares are occupied by oxygen atoms, whereas the white ones are empty. Within this picture, the reconstruction observed in Ref. [10] has been described as a rotation of the black squares, resulting in a (2×2)p4g symmetry (see Fig. 1a). This distortion preserves the shape of the black squares, while the white squares become rhomboid. A similar behavior is observed for nitrogen and carbon

* Corresponding author.

1 Present address: Physics Department, Keele University, Keele, Staffordshire ST5 5BG, UK. E-mail: pha80@keele.ac.uk

0039-6028/98/$19.00
PII: S0039-6028(98)00120-4

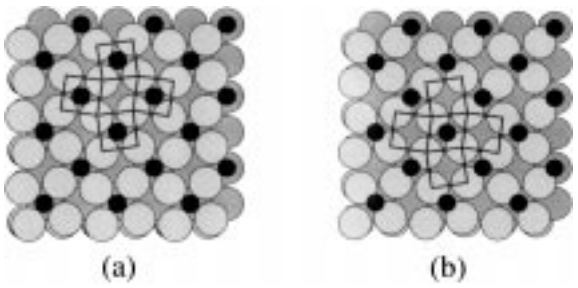

Fig. 1. Two possible clock reconstructions of the O/Rh(001) surface, resulting in a (2×2)p4g structure. In the black reconstruction (a) the squares with an O atom in the middle rotate, while the empty ones distort to rhombi. In the white reconstruction (b), the opposite occurs.

adsorbed on the (001) surface of nickel, where the rotation angle of the squares is much larger and the clock reconstruction more evident [11–14].

In this paper, we present an ab-initio study of the oxygen adsorption on the Rh(001) surface. In agreement with experimental findings, we find that the preferred adsorption site is the hollow one, at the center of the square formed by four first-layer rhodium atoms. However, at variance with recent claims based on STM experiments [10], we find that it is the white squares which rotate rather than the black ones (see Fig. 1b). In spite of this apparent discrepancy, we argue that our predicted reconstruction pattern is indeed compatible with experimental findings. In fact, the symmetry of our predicted reconstruction pattern differs slightly from what appears in the experimental STM pictures, in that adatoms get off the center of the distorted squares, thus resulting in an asymmetric clock reconstruction. The existence of two inequivalent low-symmetry sites that oxygen atoms can occupy in the rhombi should give rise to an order–disorder transition, the properties of which, however, lie beyond the scope of the present study. The amplitude of the asymmetric component of the reconstruction might be too small to be detected experimentally. Furthermore, it is likely that the temperatures at which these STM images have been taken lie above the critical temperature of transition. In order to understand the driving mechanism of the reconstruction, this is better visualized as a rhomboid deformation of the squares filled by adsorbed oxygen atoms. This distortion can then be rationalized by a simple chemical model of the re-bonding of O atoms at the surface.

2. Computational method

Our calculations are based on density functional theory within the local-density approximation [15,16], using Ceperley–Alder exchange-correlation (XC) energies [17]. The one-particle Kohn–Sham equations are solved self-consistently using plane-wave basis sets in a pseudopotential scheme. Because of the well-known hardness of the norm-conserving pseudopotentials for the O and – to a lesser extent – Rh atoms, we make use of ultra-soft pseudopotentials [18] which allow an accurate description of the O and Rh valence pseudo-wave functions with a modest basis set including plane waves up to a kinetic energy cutoff of 30 Ry. In the case of Rh, we found it convenient to treat the s and p channels using a norm-conserving potential, while the ultra-soft scheme is applied only to the hard d orbital [19–21]. Brillouin zone integrations have been performed using the Gaussian smearing [22] special-point [23] technique. We find that the structural properties of bulk rhodium are well converged using a first-order Gaussian smearing function [22] of width $s=0.03$ Ry and ten special $\boldsymbol{k}$-points in the irreducible wedge of the Brillouin zone (IBZ). The isolated surface is modeled by a periodically repeated supercell. We have used the same supercell for both the clean and the O-covered surfaces. For the clean surface, we have used five atomic layers plus a vacuum region corresponding to ~6 layers. For the O-covered surface, the five Rh layers are completed by one layer of O molecules on each side of the slab: in this case, the vacuum region is correspondingly reduced to ~5 atomic layers. We have used the same Gaussian smearing function as in the bulk calculations with a (12,12,2) Monkhorst–Pack mesh [23], resulting in 21 special $\boldsymbol{k}$-points in the (1×1) surface IBZ. Convergence tests performed with a value of s twice as small and a correspondingly finer mesh of special points resulted in no significant changes in total energies and equilibrium geometries. The latter are found

by allowing all the atoms in the slab to relax until the force acting on each of them is smaller than 0.1×10^{-3} Ry/a_0 .

3. Results

For the clean surface we find that – in agreement with other ab-initio calculations [4–9] – the first layer relaxes inward by $3.8 \pm 0.2\%$ (see Table 1), whereas the second layer is practically unrelaxed (the error is essentially a finite-size effect, and it is estimated by repeating the calculation using thicker slabs). As was noted in Section 1, the value of the first-layer relaxation reported in the experimental literature is anomalously small (the first interlayer spacing is practically equal to its bulk value within error bars). Recently, Cho and Scheffler [9] pointed out that a proper account of the vibrational contribution to the surface free energy may result in a reduction of the inward relaxation of the first layer, thus bringing theoretical predictions in better agreement with experiments. No attempts of estimating these vibrational effects have been done in the present work. Our calculated values for the surface energy s and work function w are $s \approx 1.4$ eV/atom and $w \approx 5.5$ eV (see Table 1).

Special care must be taken when estimating the latter, for the XC potential goes to zero rather slowly in the vacuum region. As the electrostatic (Hartree) potential converges much more rapidly than the XC potential to its vacuum value, it is convenient to evaluate the vacuum level by simply neglecting the XC contributions. As a preliminary study of oxygen adsorption, we performed a couple of simple ab-initio molecular dynamics simulations of an O_2 molecule impinging onto the surface. We tried two possible initial conditions for the molecule, in both of which the axis of the molecule is parallel to the surface. In the first case, the projection of the center of the molecule on the surface falls on top of a surface atom, whereas in the other, it falls on a bridge site. The initial velocity of the molecule is orthogonal to the surface, and its modulus corresponds to a temperature of 300 K, whereas the surface is initially assumed to be at zero temperature. The initial distance of the molecule from the surface is ~ 6 a.u., which is essentially in the vacuum. When the molecule arrives at the surface, the molecular bond breaks and the surface heats up. In order to find the ground-state atomic configuration, we slowly cooled the system, ending with the structure displayed in Fig. 2: the oxygen atoms adsorb in every second hollow site of the surface, resulting in a $c(2 \times 2)$ structure, where the squares whose centers

Table 1
Structural data for the three oxygenated structures investigated (see Fig. 3) and for the clean surface

Unit	d/d_0 (%)	d_{01} (Å)	d_{12}/d_0 (%)	w (eV)	$E-E_{hollow}$ (eV/at)	s (eV/at)
Clean			−3.8%	5.5		1.36
Experiment				5.0[b]		1.27[c]
			−1.2 ± 1.6%[a]			
Top		1.81	+3	7.5	+1.5	
Bridge		1.33	+0.5	6.8	+0.3	
Hollow		1.02	+0.5	6.2	+0.0	
S. clock	∼4	1.02	+0.5	6.2	−0.003	
A. clock	∼11	0.98–1.06	+0.5–0.1	6.1	−0.030	

The coverage is $\Theta = 1/2$. d_0 is the bulk lattice spacing; d_{01} is the distance between the oxygen atoms and the first rhodium layer; and d_{12} is the distance between the first and second layers. For the asymmetric clock reconstruction, the two numbers given refer to the two inequivalent first-layer rhodium atoms (see Fig. 2). d is the amplitude of the movement of the first-layer rhodium atoms upon distortion (see Fig. 3b); w is the work function; and s is the surface energy.

[a] From Ref. [3].

[b] From Ref. [24].

[c] From Ref. [25].

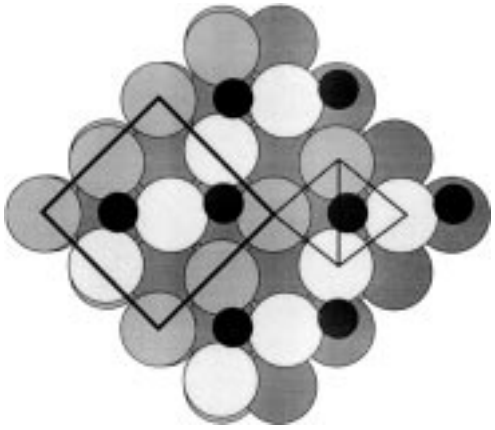

Fig. 2. Equilibrium structure of O/Rh(001) as obtained by our simulated annealing procedure. The thick line indicates the unit cell. The thin line indicates the rhombus and its shorter diagonal. The oxygen atoms are alternatively shifted orthogonally with respect to the shorter diagonal. The atoms of the first surface layer (depicted with a brighter tone) are ~ 0.08 Å higher then the others.

are occupied by an adatom are deformed into rhombi. The oxygens do not stay in the middle of the short diagonal of the rhombus thus formed, but move away in the orthogonal direction, becoming essentially three-fold coordinated. As a result of the reduced symmetry thus obtained, the atomic rows of the first Rh layer are no longer equivalent to each other: every second row is formed by atoms which have two oxygen neighbors, whereas the others have only one neighbor. As a consequence, the first rhodium layer becomes buckled, with the two-fold coordinated rows leaning ~ 0.08 Å outwards.

This asymmetric clock reconstruction can be imagined as a succession of two steps: in the first, the occupied black squares distort while the adatoms stay at the center of the rhombi (symmetric clock reconstruction); in the second, the adatom departs from the centers of the rhombi in order to achieve three-fold coordination. Both the unreconstructed and symmetric clock structures result in saddle points whose energies are reported in Table 1. We have explicitly verified that the unreconstructed structure is stable against analogous distortions affecting the white squares. For the sake of completeness, in Table 1 we also report the relative surface energies corresponding to two other adsorption sites (see Fig. 3), which are, however, much larger than the energy differences between the unreconstructed hollow structure and the corresponding clock reconstructions.

The work function is larger at a coverage $\Theta = 0.5$ than for the clean surface (see Table 1), thus indicating that electrons tend to transfer from the Rh substrate to the oxygen layer, so as to increase the surface dipole. In Fig. 4, we display the adsorption energy E_{ad} as a function of coverage Θ defined as $E_{ad}(\Theta) = s(\Theta) - s(0) - (\Theta/2)E_{O_2}$, where $s(\Theta)$ is the surface energy of the oxygen-covered system, and E_{O_2} is the energy of the isolated O_2 molecule. Coverage $\Theta = 1$ is realized by filling all the hollow sites; for $\Theta = 0.75$ and $\Theta = 0.25$, three and one of the four possible hollow sites in a (2×2) substrate supercell have been occupied. The minimum energy corresponds to a coverage in the range $0.5 \leq \Theta \leq 1$. In this range, however, the curve is very flat, and the variation of the adsorption energy (~ 100 meV) is smaller than the expected accuracy of the terms which enter its definition. All we can safely predict is that the stable coverage state lies somewhere between $\Theta = 0.5$ and $\Theta = 1$. The value of the most stable coverage is determined by a trade-off between the adsorption energy of an isolated oxygen molecule, which tends to favor a high coverage, and the oxygen–oxygen electrostatic repulsion due to charge transfer, which becomes more effective when the average O–O distance becomes smaller than some typical screening length, and which tends instead to favor a low coverage.

4. Discussion

From Fig. 2, it is evident that the oxygen sublattice forms a zigzag arrangement which is not observed in the experiments [10]. However, there are two equivalent three-fold sites for each cell occupied by an oxygen adatom, one on each side of the bridge. Neglecting the interactions between different adsorption sites, each of them is therefore two-fold degenerate. We postulate that the system undergoes an order–disorder transition at some critical temperature which depends on the magnitude of the adsorbate–adsorbate interactions, and that this temperature is lower than that at which

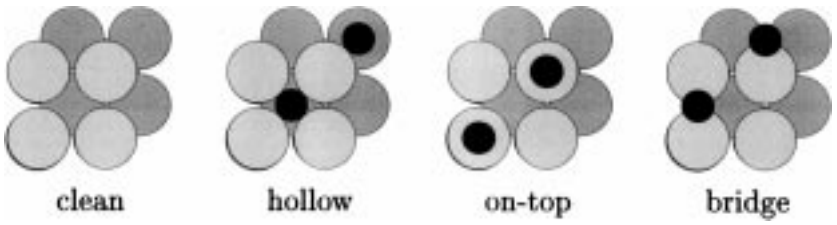

Fig. 3. Sketch of the various O adsorption sites of the Rh(001) surfaces considered in this work. Small dark circles: O atoms. Large lighter circles: first-layer Rh atoms. Large darker circles: second-layer Rh atoms.

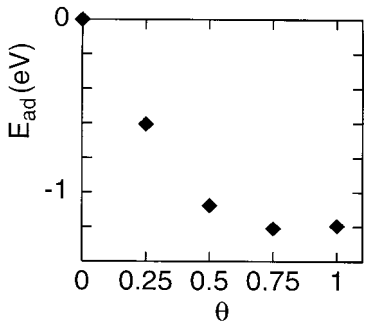

Fig. 4. Oxygen adsorption energy E_{ad} (eV), as function of coverage Θ.

the STM images were taken. The fact that no disorder in the O adlayer appears from these images indicates that the frequency of oxygen barrier crossing is much larger than the scanning frequency of the STM. This is compatible with our estimate of the barrier height ($\sim$30 meV, as obtained by comparing the energies of the symmetric clock and the asymmetric clock structures) which is of the order of the room temperature.

The STM pictures reported in Ref. [10] are such that only Rh or O atoms are visible in turn in a same picture. Because of this, it is difficult to judge whether the squares which undergo a rhomboid distortion are those filled by an adatom, or they are instead empty. What appears to be rather evident is that the distorted squares display a depletion with respect to the undistorted ones. In analogy with a similar reconstruction which is observed to occur in N/Ni(001) and which is much better characterized [26], the authors of Ref. [10] conclude that O atoms are thrust down the first Rh layer in the middle of the undistorted squares. We have simulated STM pictures using the Tersoff–Hamann model [27], but we have not been able to eliminate the images of the O atoms from any of our simulated pictures. In all of them, O atoms appear as protrusions in the middle of the distorted squares, in qualitative agreement with the experimental observation that undistorted squares are depleted with respect to the distorted ones.

In Fig. 5, we display the surface-projected densities of states (SDOS) of the clean and of the oxygen-covered Rh(001) surface, along with their decompositions into various atomic-like contributions. The SDOS of the clean surface differs from its bulk counterpart mainly because of its more pronounced narrowness due to the lower coordination of surface atoms [8,20], and it is almost entirely determined by its d-like component (see Fig. 5a). In the bulk FCC structure, the three d_{xy}, d_{xz} and d_{yz} are degenerate, and so are $d_{3z^2-r^2}$ and $d_{x^2-y^2}$. This degeneracy is partially lifted at the surface because the surface atoms lose the neighbors in the direction orthogonal to the surface. For the (001) surface, the d_{xz} and d_{yz} orbitals are still equivalent by symmetry and, hence, degenerate. The position of the oxygen atomic p-level is around 3.1 eV below the Fermi energy of the oxygen-covered surface. Inspection of Fig. 5d shows that the $O_{p_x} = O_{p_y}$ level gives rise to a bonding and an anti-bonding main peak, respectively, below (-5.8 V) and above ($+1$ eV) the Fermi level. Upon oxygen adsorption, first-layer Rh atoms become locally inequivalent according to whether the neighboring oxygen atoms are aligned along the x or y directions (see Fig. 5e). The projected densities of states (PDOS) plotted in Fig. 5d refer to those Rh atoms which have O neighbors aligned along the y direction (the PDOS of the other Rh atoms can be obtained by simply exchanging x with y). It is also easy to recognize

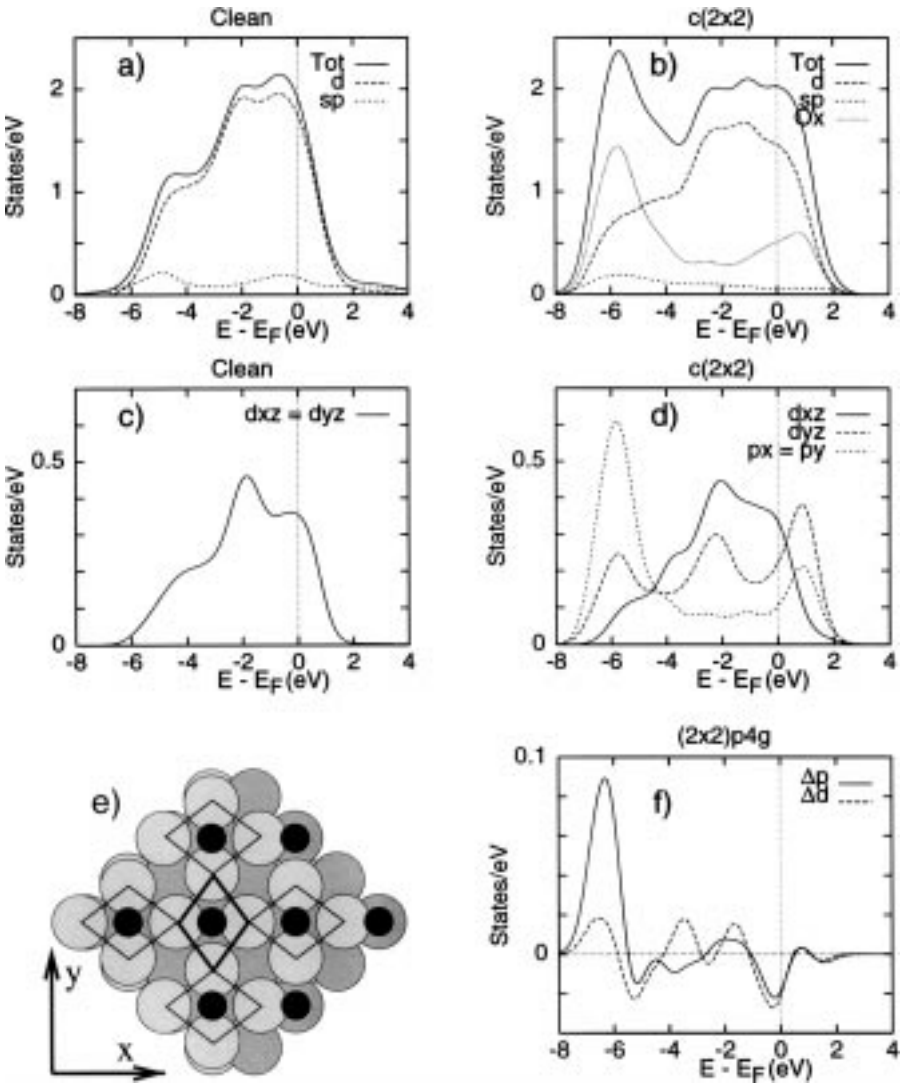

Fig. 5. (a) Surface projected density of states for the clean Rh(001) surface. (b) Surface projected density of states for the the oxygen covered one Rh(001) surface. (c) Projection of the SDOS on to the $d_{xz} = d_{yz}$ first-layer rhodium orbitals for the clean surface. (d) Projection of the SDOS on to the $p_x = p_y$ oxygen orbitals and of d_{xz} and d_{yz} first-layer rhodium orbitals for oxygenated, unreconstructed, surface. (e) Sketch of the (2×2)p4g clock reconstruction. The amplitude of the deformation is exaggerated for clarity. (f) Differences between the O_p- and Rh_d-projected density of states in the reconstructed and unreconstructed structures.

that the same bonding and anti-bonding features occur in the d_{yz} band whose atomic orbitals have lobes oriented towards the adsorbed oxygen, whereas the d_{xz} band remains similar to that of the clean surface (see Fig. 5c) because in that direction, the surface sites are empty. The O_{p_x} orbitals make bonds with the d_{xz} orbitals of the Rh atoms along the *x* direction, whereas the O_{p_y} orbitals hybridize with the d_{yz} orbitals of the Rh atoms along the *y* direction. We find that the $c(2\times2)$ structure is not the most stable one, and that a (2×2)p4g reconstruction occurs which shortens and strengthens the O–Rh bonds along one direction, while lengthening them in the perpendicular direction, as illustrated in Fig. 5e. The amplitude of the distortion depends rather sensi-

tively on the lattice parameter: using our calculated lattice parameter, we estimate the distortion to be $\sim 4\%$. If one uses a lattice parameter which is 1% larger, the amplitude of the distortion is also increased, reaching a value of $\sim 6\%$. The opposite occurs if the lattice parameter is reduced. The tendency of the system to strengthen two of the four rhodium bonds at the expenses of the other two results in a net lowering of the surface energy of ~ 3 meV/atom, thus stabilizing the (2×2)p4g structure. In the asymmetric, more stable clock structure, the size of the distortion is $\sim 11\%$ (using our calculated lattice parameter), and the surface energy gain is ~ 30 meV/atom. This shows that the reconstruction occurs because the optimal O–Rh bond length is shorter than that realized in the ideal geometry. The chemical contribution to the energy reduction which determines the distortion is illustrated in Fig. 5f, which shows the differences between the Rh_d and O_p PDOS after and before the reconstruction. In both cases, we notice a push of states towards lower energies.

5. Conclusions

Our ab-initio results confirm the experimental evidence of the dissociative character of the oxygen adsorption on Rh(001) and that the favored adsorption site is the four-fold one. A (2×2)p4g reconstruction of the surface is also predicted, in agreement with SPA-LEED data. At variance with claims based on recent STM work, we find that this reconstruction is due to a rhomboid distortion of the squares formed by first-layer Rh atoms which have an O atom adsorbed in the middle, and that this structure is unstable with respect to a departure of the adatoms from the centers of the resulting rhombi. We argue that the experimental evidence upon which these claims are founded is rather weak, and we suggest therefore that further experimental work is needed to fully characterize the reconstruction of this surface. Furthermore, we find evidence that an order–disorder transition should occur at some temperature below that at which the STM pictures have been taken. Our findings are substantiated by a simple chemical model of the mechanisms responsible for the reconstruction.

Acknowledgements

Our calculations were performed on the SISSA IBM-SP2 and CINECA-INFM Cray-T3D/E parallel machines in Trieste and Bologna respectively, using the parallel version of the PWSCF code. Access to the Cray machines was granted within the Iniziativa Trasversale Calcolo Parallelo of the INFM.

References

[1] P.R. Watson, F.R. Shepherd, D.C. Frost, K.A.R. Mitchell, Surf. Sci. 72 (1978) 562.
[2] W. Oed, B. Dötsch, L. Hammer, K. Heinz, K. Müller, Surf. Sci. 207 (1988) 55.
[3] A.M. Begley, S.K. Kim, F. Jona, P.M. Marcus, Phys. Rev. B 48 (1993) 12326.
[4] P.J. Feibelmann, D.R. Hamann, Surf. Sci. 234 (1990) 377.
[5] M. Methfessel, D. Hennig, M. Sheffler, Phys. Rev. B 46 (1992) 4816.
[6] I. Morrison, D.M. Bylander, L. Kleinmann, Phys. Rev. Lett. 71 (1993) 1083.
[7] J.-H. Cho, M.-H. Kang, Phys. Rev. B Lett. 52 (1995) 13805.
[8] A. Eichler, J. Hafner, J. Furthmüller, G. Kresse, Surf. Sci. 346 (1996) 300.
[9] J.H. Cho, M. Sheffler, Phys. Rev. Lett. 78 (1997) 1299.
[10] J.R. Mercer, P. Finetti, F.M. Leisble, R. McGrath, V.R. Dhanak, A. Baraldi, K.C. Prince, R. Rosei, Surf. Sci. 352–354 (1996) 173.
[11] W. Daum, S. Lehwald, H. Ibach, Surf. Sci. 178 (1986) 528.
[12] J.H. Onuferko, D.P. Woodruff, B.W. Holland, Surf. Sci. 87 (1979) 357.
[13] C. Klink, L. Olesen, F. Besenbacher, I. Stensgaard, E. Laegsgaard, N.D. Lang, Phys. Rev. Lett. 71 (1993) 4350.
[14] F.M. Leibsle, Surf. Sci. 297 (1993) 98.
[15] P. Hohenberg, W. Kohn, Phys. Rev. 136 (1964) B864.
[16] W. Kohn, L. Sham, Phys. Rev. 140 (1965) A1133.
[17] D. Ceperley, B. Alder, Phys. Rev. Lett. 45 (1980) 566.
[18] D. Vanderbilt, Phys. Rev. B 41 (1990) 7892.
[19] K. Stokbro, Phys. Rev. B 53 (1996) 6869.
[20] K. Stokbro, S. Baroni, Surf. Sci. 370 (1997) 166.
[21] D. Alfè, S. Baroni, Surf. Sci. 382 (1997) L666.
[22] M. Methfessel, A. Paxton, Phys. Rev. B 40 (1989) 3616.
[23] H.J. Monkhorst, J.D. Pack, Phys. Rev. B 13 (1976) 5188.
[24] CRC Handbook of Chemistry and Physics, 67th ed., CRC Press, Boca Raton, FL, 1987.
[25] L.Z. Mezey, J. Giber, Jpn. J. Appl. Phys. 21 (1982) 1569.
[26] L. Wenzel, D. Arvanitis, W. Daum, H.H. Rotermund, J. Stohr, K. Baberschke, H. Ibach, Phys. Rev. B 36 (1987) 7689.
[27] J. Tersoff, D.R. Hamann, Phys. Rev. B 31 (1985) 805.